Multistage Pulse Tube Refrigeration Characterization of the Lockheed-Martin RAMOS Cryocooler

W. Scheirer, T. Roberts, and E. Pettyjohn

Air Force Research Laboratory
Kirtland AFB, NM, USA 87117

ABSTRACT

The performance mapping of a multistage pulse tube refrigeration system has been performed on the Lockheed Martin RAMOS cryocooler by the Air Force Research Laboratory (AFRL). The results are presented in terms of primitive variables such as temperature, work inputs, and cooling load supported. It is then restated in terms of composite variables such as available work (exergy) inputs, the individual and composite exergies of the cooling loads supported, and system efficiency. Additional data from the heat rejection interfaces of this refrigeration system are presented, including the temperature variations over the extended compressor-expander section transfer line. The data presented shows both the application envelope of this refrigerator and how it interacts with its application environment.

INTRODUCTION

The Russian American Military Observation Satellite (RAMOS) payload procurement program was terminated by the Missile Defense Agency and the residual cryocooler asset was transferred to AFRL in 2006. The cryocooler and rack control electronics were completed by Lockheed Martin (Palo Alto, CA) on a low cost effort and delivered as shown in Figure 1. The cryocooler is a two-stage pulse tube with a nominal design point of :

Total Input Power Including Electronics: 125W

Operating Frequency: 54 Hz	Rejection Temperature: 300 K
1st stage ("mid"): 6W at 130K	2nd stage ("tip"): 0.75W @ 75K

The rejection interface is defined as the base of the compressor mechanical support, a fairly substantial aluminum fixture. The pulse tube base plate is also cooled in parallel, but its temperature was not controlled as was the compressor mount. The difference between these rejection points was less than 10 K.

CHARACTERIZATION RESULTS

The normal cooldown curve for a near 300 K rejection temperature is shown in Figure 2, and this curve's nature did not change throughout the characterization program. After verifying a stable no-load condition, the nominal design point was verified and a operational frequency survey was

Cryocoolers 15, edited by S.D. Miller and R.G. Ross, Jr.

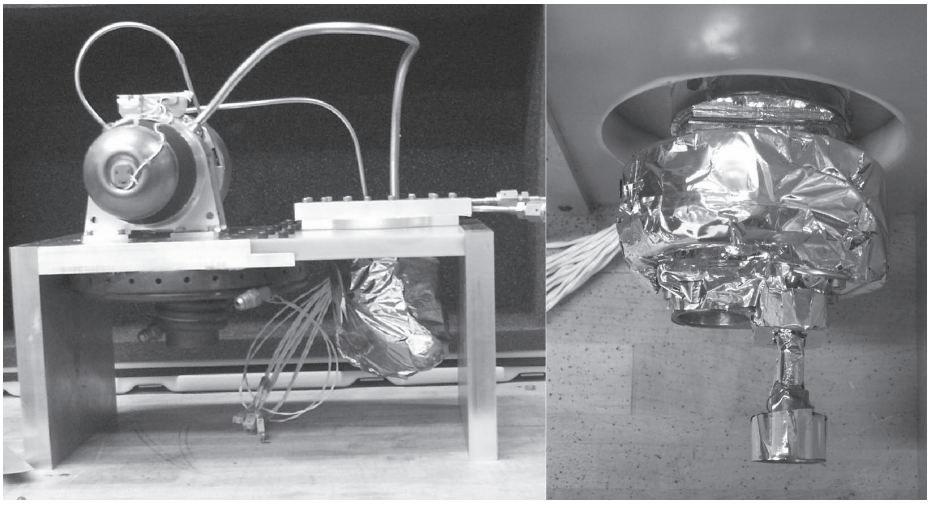

Figure 1. Overall cryocooler configuration, compressor to the right, large piping is the compressor-pulse tube transfer line, smaller piping is the pulse tube inertance tube, The compressor housing serves as the reservoir at the end of the inertance tube. The inertance tube is wrapped 10 times around the compressor housing. The mechanical pedestal of the compressor is the thermal rejection path for the compressor; the rejection path for the expander base is that base itself. To the right is shown the two cooling stage cold blocks. The regenerator and pulse tube for the upper stage, and inertance tube and reservoir for the lower stage, are obscured by MLI.

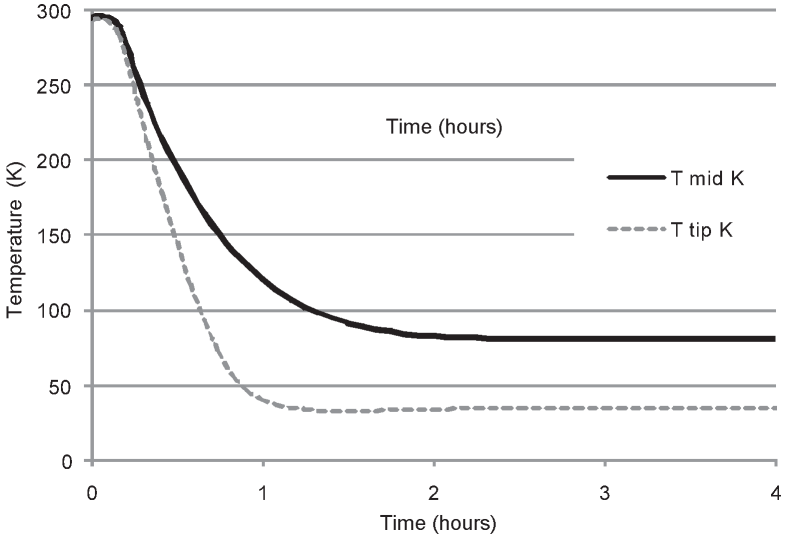

Figure 2. 54 Hz cooldown curves with steady state at 3 hours; rejection to 297.6 K.

commenced at a 300 K rejection temperature. The data line in Figure 3 denoted "300 K-Sep07" was the result of this survey, confirming the nominal design point's operating frequency was optimal. The other Figure 3 results will be discussed below.

Performance Mapping

A baseline performance loadline was conducted to indicate performance in "as delivered" condition, and is shown in Figure 4. This line had no load on the tip and varied the load on the mid

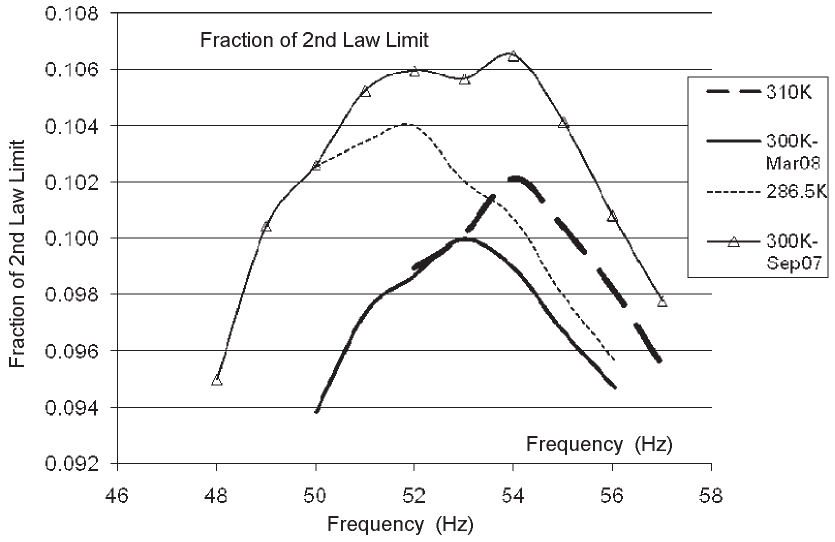

Figure 3. Results of performance scan at various frequencies and rejection temperatures. Note the shift in performance between the data for Sept. 2007 and Mar. 2008.

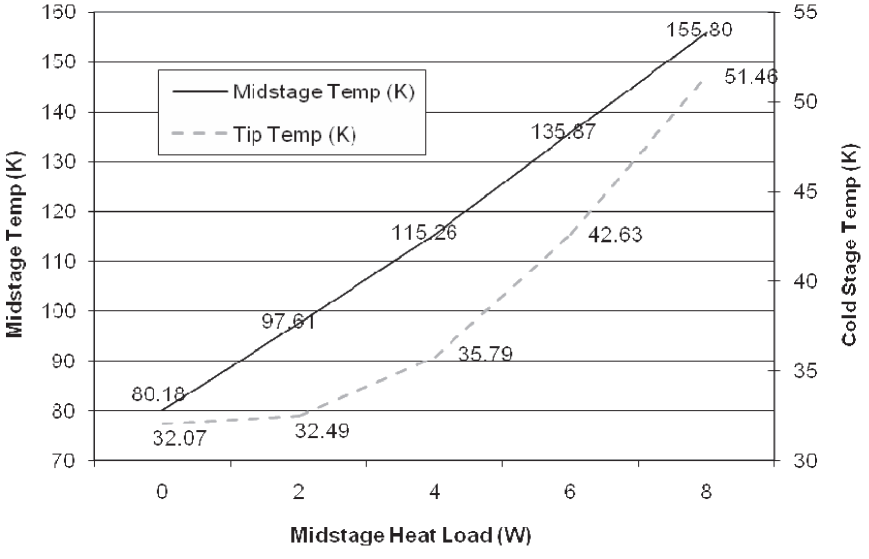

Figure 4. Baseline loadline at rejection = 300K, 54 Hz.

stage from 0 to 8 W. A more extensive mapping was then done, with results in Figure 5 and Table 1. The general trends shown were entirely consistent with design expectations and showed superior performance when supporting larger loads at higher temperatures, as indicated by the higher values of "Carnot fraction" (i.e. fraction of 2nd Law limit) in Table 1.

How operating frequency affected this overall performance map is indicated in Figure 6, with exergetic cooling defined for an *n* stage cooler as:

$$Q_{exergetic} = \sum_{i=1}^{n} \left(Q_{cooling,i} \frac{T_{rej} - T_{cooling,i}}{T_{cooling,i}} \right) \quad (1)$$

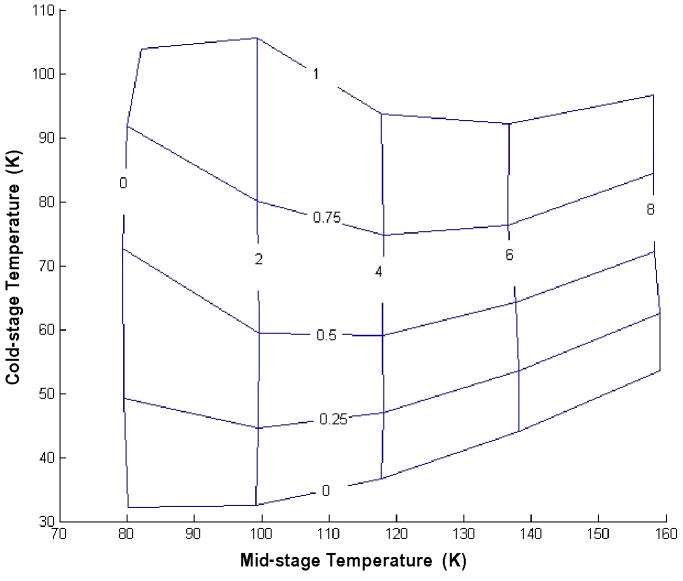

Figure 5. Overall cryocooler performance mapping at rejection = 300K.

Table 1. Performance mapping data at rejection = 300 K.

Diode 1	Diode 2	Pi (W)	TR (K)	QL1 (W)	QL2 (W)	Oper Freq (Hz)	Cooling Exergy (W)	Carnot fraction
80.18	32.07	90.45	299.86	0	0	54	0.0000	0.0000
99.20	32.50	92.88	299.96	2	0	54	4.0476	0.0436
117.70	36.61	93.25	299.96	4	0	54	6.1937	0.0664
138.20	44.04	91.83	299.86	6	0	54	7.0186	0.0764
159.11	53.48	90.16	299.96	8	0	54	7.0820	0.0785
79.60	49.19	91.47	299.86	0	0.25	54	1.2741	0.0139
99.51	44.53	93.90	300.06	2	0.25	54	5.4651	0.0582
118.04	46.99	93.50	300.06	4	0.25	54	7.5144	0.0804
138.26	53.56	92.18	299.96	6	0.25	54	8.1671	0.0886
159.12	62.42	90.35	300.06	8	0.25	54	8.0382	0.0890
79.35	72.63	92.43	299.96	0	0.5	54	1.5650	0.0169
99.68	59.37	93.64	299.96	2	0.5	54	6.0446	0.0645
117.89	59.07	94.31	300.06	4	0.5	54	8.2203	0.0872
137.72	64.18	92.29	299.96	6	0.5	54	8.9056	0.0965
158.36	72.15	91.36	300.16	8	0.5	54	8.7434	0.0957
80.05	91.84	92.97	299.96	0	0.75	54	1.6996	0.0183
99.32	80.06	94.72	300.06	2	0.75	54	6.1032	0.0644
118.04	74.66	93.87	300.06	4	0.75	54	8.4327	0.0898
136.59	76.38	93.38	299.96	6	0.75	54	9.3721	0.1004
158.04	84.39	91.80	300.16	8	0.75	54	9.1117	0.0993
82.14	103.91	93.15	299.96	0	1	54	1.8867	0.0203
99.29	105.57	95.25	300.06	2	1	54	5.8867	0.0618
117.72	93.71	94.64	300.06	4	1	54	8.3980	0.0887
136.66	92.09	93.39	300.06	6	1	54	9.4327	0.1010
158.12	96.56	92.02	300.16	8	1	54	9.2954	0.1010

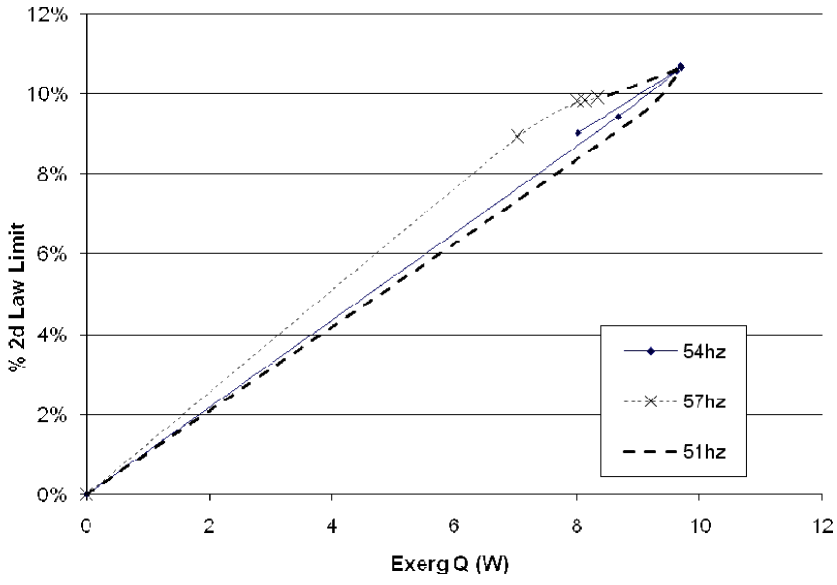

Figure 6. Exergetic cooling performance mapping at rejection = 300K.

The general performance path of Table 1's data is labeled "54 Hz" and shows a fairly narrow looped path characteristic of pulse tube performance at optimal operating frequency. Taking the cooler 3 Hz off optimal frequency produces interesting effects. Not depicted is the fact that the no-load 51 Hz temperature is slightly lower than at 54 Hz. The 51 Hz loop however shows generally slightly lower efficiency and cooling supported in almost all cases. This correlates with the shallow degradation with respect to frequency shown in Figure 3 for 300 K's data for 54 and 51 Hz. The 57 Hz data is more curious. It shows a distinct capacity degradation from 54 Hz peformance, but it is more efficient, and at very high loads is close to the 54 Hz. This 57 Hz data would seem to suggest that the 57 Hz frequency becomes closer to optimal as the cooling loads increase and exceed 1 W at the tip and 6 W at the mid stage.

Temporal Shifts in Performance

Over a 24 hour period the RAMOS cooler exhibited acceptable temperature stability when run open loop at constant cooling loads. It was noticed during performance mapping that leaving the cooler on overnight at no load resulted in shifts in performance over several days. The performance mapping was therefore done with shutdowns every night. After that mapping the frequency survey in Figure 3 was performed with the data lines for 310 K, 286.5 K, and 300 K-Mar08 sequentially obtained over a three week period, with continuous operation. The noticeable degradation of the 300 K performance compared to the Sept. 2007 data indicated that some temporal degradation was affecting performance, although the conclusion available from the data in Figure 3 that rejection temperature affects optimal operating frequency is still valid.

Using Occam's Razor, the simplest explanation for this performance shift was a contaminated working fluid, and testing that hypothesis was simple. The cooler was left off for 5 days at 310 K, and then performance data from Sept. 2007 (after nightly shutdowns), 25 Mar. 2008 (after long continuous runtime) , and 31 Mar. 2008 (after shutdown), were compared. The results are shown in Figure 7. The 25Mar08 data is after three weeks run time and the 31Mar08 data is after the five day shut down. It can be clearly seen that the 31Mar08 data nearly returned to the data taken in Sept. 2007. This return to original performance without hysteresis also implies that no stiction effects are significantly creating this shift in performance.

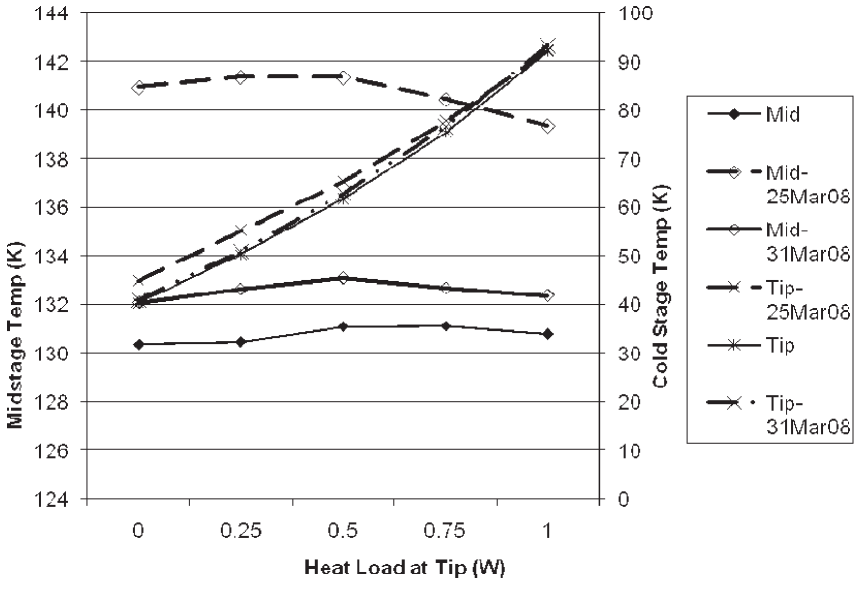

Figure 7. Loadline shifts at rejection = 300K, 54 Hz, 6W at mid stage.

The characterization program was consequently terminated as the data obtained, while indicative of overall performance trends, could only be interpreted under the strong caveat that it was affected by non equilibrium thermodynamic conditions.

TRANSFER LINE AND INERTANCE TUBE TEMPERATURE DISTRIBUTIONS

As the RAMOS cooler is the first Stirling variant cooler to be received at AFRL with a distinct separation of the compressor and pulse tube sections, some estimate of the irreversibilities caused by this separation was desired, along with a description of the flow fields' boundary conditions in the transfer line and the second stage inertance tube to support future CFD modeling efforts. This goal was accomplished by measuring temperature gradients along the compressor-pulse tube expander transfer line and along the inertance tube. These gradient measurements do not require a stable thermodynamic equilibrium, which the contaminated working fluid would prevent. Instead they represent snap shots of refrigeration system interactions with its environment. From these temperature measurements certain conclusions can be made concerning:

a. The internal irreversibilities occuring in these refrigerator components.

b. The nature of the boundary conditions on refrigerator operation.

c. How the internal operation of the refrigerator is affected by acoustic wavelengths versus operating frequency variations.

From these conclusions, suggestions for improved refrigerator operation and design can be derived.

Anticipated Results

The loads in this experiment are defined in Table 2. Due to prior experience with Stirling-cycle refrigerators of various sorts, it was known that transfer lines and inertance tubes "got hot," and were far from perfect thermodynamic devices. This experiment therefore sought to measure how the actual items on the RAMOS cooler behaved differently from the known, quadratic solution to the energy equation for these plumbing lines for a constant heat flux/unit length and known endpoint temperatures. If substantive differences from the "expected" quadratic solutions were noted, then prior modeling work which anticipated such differences would be confirmed.

Table 2. Experimental loads

Q-low stage	Q- mid stage	Total Exergetic Q (@54 Hz)	Q (@51 Hz)
0 W	0 W	0.0 W	0.0 W
0.75 W	4 W	8.671 W	8.990 W
0.75 W	6 W	9.695 W, 9.685 W	9.657 W
1 W	6 W	9.616 W	9.644 W
1 W	8 W	8.104 W	8.460 W

Transfer Line Results

Three different sets of data were obtained on equally spaced thermocouples on the compressor-pulse tube base transfer line for 51.02, 54.00, and 56.95 Hz. The results for 51 and 54 Hz are shown in Figures 8 and 9. It can immediately be noted that these temperature curves are not quadratic in nature. Most rise linearly for over half the length of the tube and then are concave downwards for the last half. With the exception of no-load (zero exergetic cooling) lines, most have maxima close to the pulse tube end. Some of the other differences in these plots might be explained by the performance shifts of the cooler itself as it supports higher loads at higher temperatures. The relevance of the system performance to transfer line operating conditions is in that how the transfer line is acting as a conduit for *Pdv* acoustic power waves to the pulse tube from the compressor. For these changing conditions, not only are the operating wave interactions changing, but the nature of the pulse tube expander receiving those waves is changing. Over the performance envelope tested, the low stage varied over approximately 30-110K and the upper stage over 80-160K. Consequently, the effective fill pressure, speed of sound, and viscosities of the working fluid all changed as well. These alterations would lead towards systemic impedance alterations which are probably highly significant, and would present a fertile issue to investigate in future modeling efforts. Surprising was the fact that frequency shifts from 51 to 57 Hz appeared to not radically change these results.

What we can see here are certain cases showing strong temperature maxima on the transfer line, which imply that significant irreversible losses are occurring. Conversely, some cases show almost linear temperature distributions, and these cases are usually associated with cooling loads well off

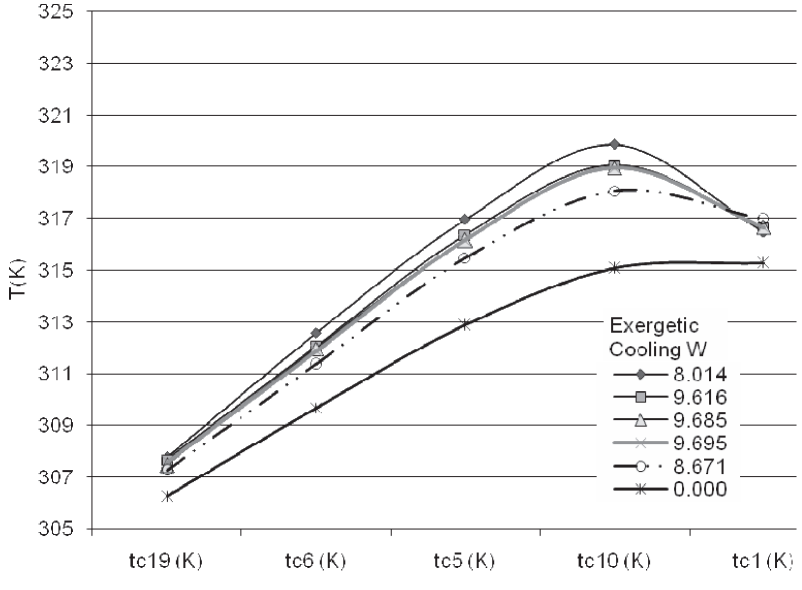

Figure 8. Transfer line temperature profile for equally spaced TCs, 54 Hz, rejection = 300K. TC 19 is at Compressor, TC 1 is at Pulse Tube heat exchange interface. Exergetic cooling lines for 9.616, 9.685, and 9.695 W are virtually superposed.

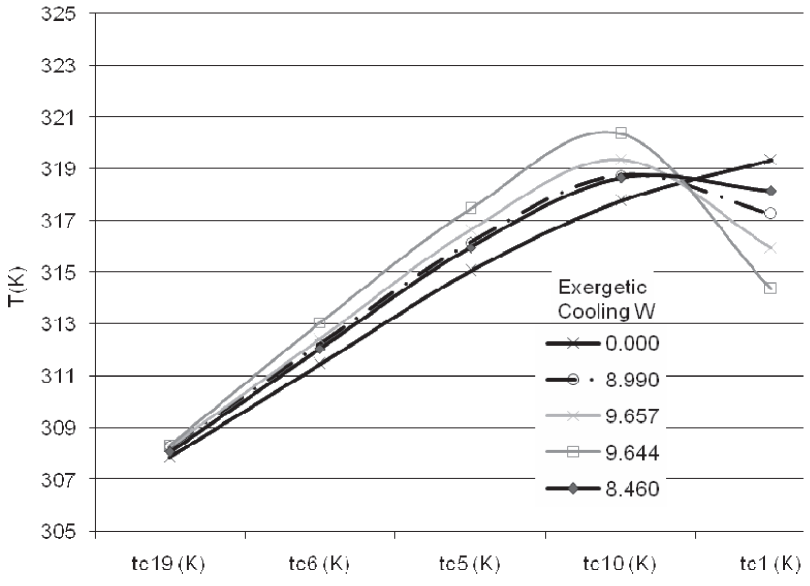

Figure 9. Mid stage inertance line temperature profile for equally spaced TCs, 54 Hz, rejection = 300K. TC 3 is at Pulse Tube heat exchange interface, TC 13 is at Compressor (reservoir). Uses same legend as Figure 8. Exergetic cooling lines for 9.616, 9.685, and 9.695 W are virtually superposed.

the system's maximum efficiencies or cooling outputs (i.e., well away from the right hand bend in the performance curves). As the latter cases are those that exhibit systemic inefficiencies, while the former are systemically efficient, it is curious that strong local inefficiencies in the transfer line happen to strongly correlate directly with high system efficiency. It is obvious, however, that the lack of transfer line inefficiency correlates also with much more significant inefficiencies elsewhere, such as in the regenerator in the no-load cases.

Inertance Tube Results

The importance of the inertance tube to pulse tube operation is that it essentially tunes the pulse tube's phase shift in mass flow rate versus acoustic pressure so that cooling loads can be maximized. It does this by possessing the correct flow resistance, capacitance, and inertia (comparable to how an AC electrical circuit is tuned with respect to its RCL impedance characteristics). Due to this complex impedance nature, a certain level of real and imaginary thermodynamic irreversibilities are to be expected, and therefore one might guess on a first order basis that these real heating effects would be constant through the length of the inertance tube. That guess would be incorrect, based on the data gathered by this experiment, see Figures 10 and 11. As with the transfer line, the inertance tube shows wide variations in its temperature profile related to overall system efficiency and operating conditions. Again, higher temperature profiles and component irreversibilities appear directly correlated to system efficiency.

CONCLUSIONS

Overall the RAMOS cooler performed well across an extended performance envelope on both stages and is well suited to electro-optical sensors requiring focal plane and optic-train cooling. The short-term performance stability (less than 24 hours) was satisfactory; however, the probable contaminated working fluid makes long-term stability of the mechanical elements hard to estimate. To attain that goal, the RAMOS will be run in a no-load condition continuously to show if the contamination effect achieves some asymptotic level. If so, then continuous runtime at no load will offer insight into other degradation processes over several years.

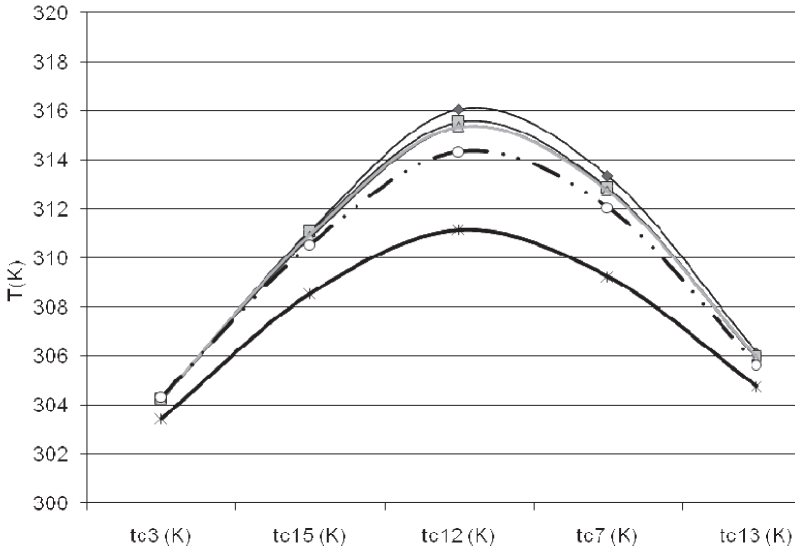

Figure 10. Transfer line temperature profile for equally spaced TCs, 51 Hz, rejection = 300K. TC 19 is at Compressor, TC 1 is at Pulse Tube heat exchange interface.

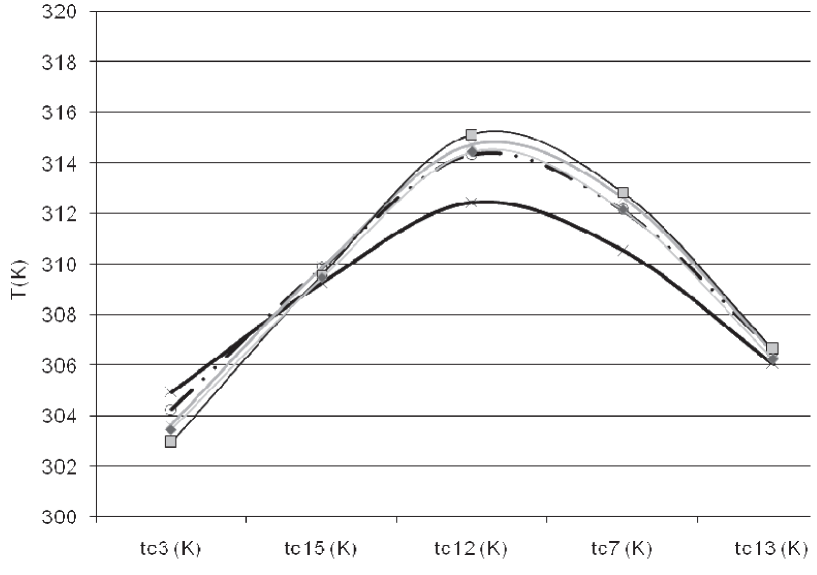

Figure 11. Mid stage inertance line temperature profile for equally spaced TCs, 51 Hz, rejection = 300K. TC 3 is at Pulse Tube heat exchange interface, TC 13 is at Compressor (reservoir). Uses same legend as Figure 10. Exergetic

REFERENCE

1. Frank, D. et al, "Lockheed Martin RAMOS Engineering Model Cryocooler," *Cryocoolers 13*, Springer Science+Business Media, New York (2005), pp. 115-120.